

# UC Berkeley

## UC Berkeley Previously Published Works

### Title

The Role of Atmospheric Rivers on Groundwater: Lessons Learned From an Extreme Wet Year

### Permalink

<https://escholarship.org/uc/item/425063sk>

### Journal

Water Resources Research, 59(6)

### ISSN

0043-1397

### Authors

Siirila-Woodburn, Erica R

Dennedy-Frank, P James

Rhoades, Alan

et al.

### Publication Date

2023-06-01

### DOI

10.1029/2022wr033061

### Copyright Information

This work is made available under the terms of a Creative Commons Attribution License, available at <https://creativecommons.org/licenses/by/4.0/>

Peer reviewed





# Water Resources Research®



## RESEARCH ARTICLE

10.1029/2022WR033061

# The Role of Atmospheric Rivers on Groundwater: Lessons Learned From an Extreme Wet Year

Erica R. Siirila-Woodburn<sup>1</sup> , P. James Dennedy-Frank<sup>1</sup> , Alan Rhoades<sup>1</sup> , Pouya Vahmani<sup>1</sup> ,  
Fadji Maina<sup>2</sup> , Benjamin Hatchett<sup>3</sup> , Yang Zhou<sup>1</sup> , and Andrew Jones<sup>1,4</sup> 

<sup>1</sup>Earth and Environmental Sciences Area, Lawrence Berkeley National Laboratory, Berkeley, CA, USA, <sup>2</sup>NASA Goddard Space Flight Center, Greenbelt, MD, USA, <sup>3</sup>Desert Research Institute, Reno, NV, USA, <sup>4</sup>Energy and Resources Group, University of CA, Berkeley, Berkeley, CA, USA

### Key Points:

- A coupled hydrologic model is forced by a regional climate model to examine the role of atmospheric rivers (ARs) on groundwater dynamics
- Tracking of atmospheric features and subsurface Lagrangian particles is used to follow the full lifecycle of water through a record wet year
- The most significant difference in AR-sourced precipitation is on the groundwater recharge-snow relationship

### Supporting Information:

Supporting Information may be found in the online version of this article.

### Correspondence to:

E. R. Siirila-Woodburn,  
[erwoodburn@lbl.gov](mailto:erwoodburn@lbl.gov)

### Citation:

Siirila-Woodburn, E. R., Dennedy-Frank, P. J., Rhoades, A., Vahmani, P., Maina, F., Hatchett, B., et al. (2023). The role of atmospheric rivers on groundwater: Lessons learned from an extreme wet year. *Water Resources Research*, 59, e2022WR033061. <https://doi.org/10.1029/2022WR033061>

Received 16 JUN 2022  
Accepted 21 APR 2023

**Abstract** In the coastal regions of the western United States, atmospheric rivers (ARs) are associated with the largest precipitation generating storms and contribute up to half of annual precipitation, but the impact of ARs on the integrated hydrologic cycle, specifically on groundwater storage and hydrodynamics, is largely unknown. To better explore the hydrologic behavior of AR versus non-AR event precipitation, we present a novel combination of two water tracking methods (one in the atmosphere and one in the subsurface) to explicitly track the full lifecycle of water parcels generated by ARs. Simulations of northern California's Cosumnes River watershed during the record wet 2017 water year are performed via the coupling of a high-resolution regional climate model and a land surface-groundwater model accounting for lateral groundwater flow. Despite ARs contributing more precipitation than non-AR storms, we find less AR water is preferentially stored in aquifers by year end. Fractionally, ARs result in 300% less snow derived groundwater-recharged compared to non-AR precipitation. Rain-on-snow (RoS) plays an important role in AR-driven discharge, where over 50% of total discharge from ARs snow is from RoS events. Finally, despite record-breaking annual precipitation, simulated groundwater depletion occurs by year end due to estimates of groundwater pumping activities. The results from these simulations serve as a partial analogue of future hydrologic conditions where ARs are expected to intensify and provide a greater fraction of annual precipitation due to climate change.

## 1. Introduction

Since the mid-2000s, atmospheric rivers (ARs) have been recognized as important sources of moisture transport that supply water resources to many regions across the globe, including the west coast of the United States, the central and northeastern regions of the United States, Australia, South Africa, South America, and western Europe (Lavers & Villarini, 2015; Neiman et al., 2008; Ralph et al., 2006; Rutz et al., 2014). These synoptic-scale atmospheric features, characterized by long and narrow concentrated moisture transport (several of thousands of km long, and typically an order of magnitude lower width) carry massive amounts of water comparable to some of the largest rivers in the world (Payne et al., 2020; Ralph, Iacobellis, et al., 2017; Zhu & Newell, 1994). In California, for example, ARs contribute 20%–50% of the state's precipitation and streamflow (Dettinger et al., 2011) and have gained traction in the scientific and water management communities as being important drivers of annual precipitation (Ralph, Dettinger, et al., 2017). The role which ARs play in contributing to annual precipitation totals may also be intensified under a warming climate, where several studies point to the Clausius-Clapeyron relationship which suggests enhanced intensity of AR-related precipitation under climate change (Gao et al., 2015; Gershunov et al., 2019; Michaelis et al., 2022; O'Brien et al., 2022; Patricola et al., 2022; Payne et al., 2020; Radić et al., 2015; Rhoades et al., 2021; Rhoades, Jones, Srivastava, et al., 2020; Shields & Kiehl, 2016). Despite the significance of ARs in augmenting current and future water resources, little is known about how AR dynamics impact the above- and below-ground hydrologic cycle, including groundwater resources.

Globally, groundwater accounts for approximately one third of freshwater resources, and is an especially important reserve during periods of drought (Famiglietti, 2014; Meixner et al., 2016). A number of AR characteristics (such as intensity and landfall duration) pose the potential to impact groundwater recharge and flow dynamics, but given potentially convoluting factors and uncertainties regarding the underlying mechanisms controlling AR-driven groundwater dynamics, little is known to what extent. Most obviously, AR occurrences result in higher intensity precipitation events, which can change groundwater infiltration rates, and lead to greater runoff ratios

© 2023. The Authors.

This is an open access article under the terms of the [Creative Commons Attribution License](https://creativecommons.org/licenses/by/4.0/), which permits use, distribution and reproduction in any medium, provided the original work is properly cited.

(i.e., a higher fraction of precipitation which results in streamflow). ARs are also known to bring about warmer atmospheric conditions, resulting in higher snow levels and more rain than snow compared to non-AR precipitation events (Hatchett et al., 2017). This change in precipitation partitioning may directly impact groundwater recharge, because snowmelt more effectively infiltrates into the subsurface when compared to rainfall (Earman et al., 2006). Changes in precipitation phase partitioning may also lead to more rain-on-snow (RoS) events, also associated with AR conditions (Chen et al., 2019; Guan et al., 2016; Michaelis et al., 2022), potentially exacerbating the effects of less snowfall on groundwater recharge. Seasonally, increased occurrence of ARs may indicate a sharpening of the winter precipitation season, so that peak hydrologic water availability would occur earlier in the water year when potential evapotranspiration is lower, potentially resulting in less overall water flux back to the atmosphere.

Very few studies have investigated the role in which ARs play on hydrologic processes, and those which do solely focus on *above-ground* hydrology. Konrad and Dettinger (2017) found that high integrated vapor transport (IVT) conditions associated with ARs coincided with the highest streamflow events between 1945 and 2015. Chen et al. (2019) similarly found that ARs produced higher streamflow than non-AR events, where runoff ratios were double that of non-AR runoff ratios if snowpack existed before the onset of the AR. They also found that RoS events during ARs are mostly driven by changes in air temperature (and to a lesser degree radiation changes) so that ARs suppress evapotranspiration.

Studies which assess changes to subsurface hydrology are even less prevalent in the literature, in part due to limitations in tracking methods, both in observational networks and numerically in model frameworks. This is despite observed relationships between antecedent soil moisture and AR-related discharge (Haleakala et al., 2022; Ralph et al., 2013). One study developed a water tracer model within the Noah LSM and found that a large fraction of precipitation from a simulated AR in the Pacific Northwest was retained in the soil after 6 months (Hu et al., 2018). However, the influence of ARs on deeper groundwater recharge rates and water storage remains a void in the hydro-meteorological and water resource communities. To the best of our knowledge, this study is the first to examine the role in which ARs contribute to groundwater dynamics.

Here, we combine two novel water tracking algorithms—above and below ground—to explore how ARs influence the integrated hydrologic cycle, with specific foci on groundwater recharge and subsurface flow. AR and non-AR precipitation is tracked across the entire atmosphere through bedrock continuum during an extreme wet year characterized by multiple ARs. We employ cutting-edge atmospheric and hydrologic simulations in high resolutions over an unimpaired watershed in northern California characterized by natural river flows. The novel coupling of above- and below-ground AR water tracking enables an examination of the full lifecycle of water. Information on AR contributions to groundwater (including water residence times, depth, and recharge timing), water source (rain vs. snow), and eventual exit pathway (evapotranspiration or discharge) are therefore all possible in this approach. This study builds on a wealth of developments in AR-tracking capabilities (Inda-Díaz et al., 2021; Rutz et al., 2019; Shields et al., 2018; Zhou et al., 2021). Similarly, subsurface tracking capabilities also have a rich history (Salamon et al., 2006) which were only recently extended to include surface processes (Bearup et al., 2016; de Rooij et al., 2013; Maxwell et al., 2019; Yang et al., 2021) with relatively few applications (Bearup et al., 2016; Maxwell et al., 2019; Wilusz et al., 2020; Yang et al., 2021), but have yet to be extended as done in this study to track individual storms or classes of storms. The cross-disciplinary approach employed here enables a physics-based understanding of the role in which atmospheric processes such as ARs have in shaping subsurface flow processes at local- and watershed-scales, relevant for decision makers and stakeholders who are adapting to rapidly changing environmental conditions (Siirila-Woodburn et al., 2021). This study also serves as a first demonstration of individual storm tracking from atmosphere through bedrock to understand water partitioning behavior which may be important to understand in a no-analogue future climate.

In addition to demonstrating these modeling tools in a new, storm-based atmosphere to groundwater framework, we seek to study the role of ARs on hydrology and to gain key lessons learned by studying a recent, extreme winter in the context of the following science questions:

- Does water derived from AR and non-AR precipitation partition differently?
- Specifically, does the character of AR precipitation events impact groundwater storage differently than non-AR precipitation? Considerations include more prolonged and higher precipitation totals, impacts from rain-snow events, and different spatial distributions of precipitation.
- And finally, what are the implications on groundwater storage dynamics and water resources?

## 2. Site Description and Selected Water Year

The Cosumnes watershed (Figure 1a) located in northern California, spans the western slope of the Sierra Nevada and terminates in the Sacramento Central Valley, similar to many watersheds in California that supply water down gradient for domestic, agricultural, or industrial water users across the state. The Cosumnes River is unique in that it is one of the last major rivers in the western United States without a major dam, enabling the rare study of uninhibited natural river flows. The Cosumnes supports some of the last remaining wetland and riparian habitat in the Sacramento Central Valley as well as a burgeoning viticultural economy and other agricultural production. An integrated hydrologic model of the Cosumnes watershed has been developed with the ParFlow-CLM model, and used to explore a myriad of above- and below-ground watershed dynamics including drought whiplash (Maina, Siirila-Woodburn, Newcomer, et al., 2020), wildfires (Maina & Siirila-Woodburn, 2019) modeling impacts due meteorological forcing resolution (Maina, Siirila-Woodburn, & Vahmani, 2020), and projections of end-of-century hydrologic states (Maina et al., 2021). A series of model validation exercises have been conducted to test the model ability to represent key hydrologic processes. Model performance has been compared to point measurement of observed streamflow and groundwater levels (see Maina, Siirila-Woodburn, Newcomer, et al., 2020; Figure 3) over recent wet and dry periods in the region. We have also conducted spatially distributed comparisons of key hydrologic variables (evapotranspiration, soil moisture, and snow water equivalent) using a variety of remote sensing products including METRIC, SMAP, SNODAS, and a MODIS-derived snow product, ParBal (see Figure 4 of Maina, Siirila-Woodburn, Newcomer, et al., 2020). Further description of the ParFlow-CLM model is described in Section 3.2.

Water year 2017 (hereafter WY2017, which spans 1 October 2016 to 30 September 2017) was selected for this study as it was the most active AR season since, at least, the mid-twentieth century (Gershunov et al., 2017). In the Cosumnes, WY2017 resulted in the highest cumulative streamflow in a >100 years record (Figure 1c), providing an opportunity for “lessons learned” from an end-member precipitation year. Although a larger sample of ARs is most ideal to assess the statistical representation of individual storms, WY2017 provides an example of different storm types typical of AR conditions in the region, and the subsequent water partitioning associated with those storms.

## 3. Methods

A combination of high-fidelity, high-resolution models and tracking techniques are used here to study the movement of water across the bedrock-through-atmosphere interface. This approach (a conceptual model is shown in Figure 2) includes feature tracking in the atmosphere to identify ARs (described in Section 3.1) and discrete particle tracking of parcels of water in the subsurface (described in Section 3.2).

### 3.1. Atmospheric Simulation and AR Tracking

The Weather Research and Forecasting model (WRF; Skamarock & Klemp, 2008; Skamarock et al., 2008) is a state-of-the-art, fully compressible, non-hydrostatic, mesoscale numerical weather prediction model. A nested domain configuration of WRF (version 3.6.1) is used to downscale NLDAS-2-based forcings to 500 m resolution. Four domains with horizontal resolutions of 13.5, 4.5, 1.5, and 0.5 km are used with 30 vertical atmospheric levels. WRF is initialized using post-spin-up soil moisture from ParFlow-CLM. Other WRF initial conditions are based on NLDAS-2 as described in Maina, Siirila-Woodburn, and Vahmani (2020). The physics parametrizations used in WRF include the Dudhia scheme (Dudhia, 1989) for shortwave radiation, the Rapid Radiative Transfer Model (Mlawer et al., 1997) for longwave radiation, University of Washington Boundary Layer Scheme (Bretherton & Park, 2009) for the planetary boundary layer, the Morrison double-moment scheme (Morrison et al., 2009) for microphysics, and the Eta Similarity scheme (Monin & Obukhov, 1954) for the model surface layer. The Grell-Freitas cumulus parameterization (Grell & Freitas, 2014) is used only for domains d01 and d02. The adopted WRF configuration has been extensively validated in the literature (Vahmani & Jones, 2017; Vahmani et al., 2019). These studies show a reasonable performance for WRF over California, reproducing daily air temperature and evapotranspiration with RMSDs of 1.1°C and 0.74 mm/day, respectively. One-way coupling of the highest resolution (0.5 km) WRF output to ParFlow-CLM was recently done as part of an analysis to quantify forcing resolution biases on integrated hydrologic processes (Maina, Siirila-Woodburn, & Vahmani, 2020) and is extended for use here to track ARs. A comparison of spatially distributed, high-frequency precipitation and temperature in the Cosumnes was performed for the WY2017 forcing used in the study, and is detailed in Appendix 4 of Maina, Siirila-Woodburn, and Vahmani (2020), showing good agreement with observations.

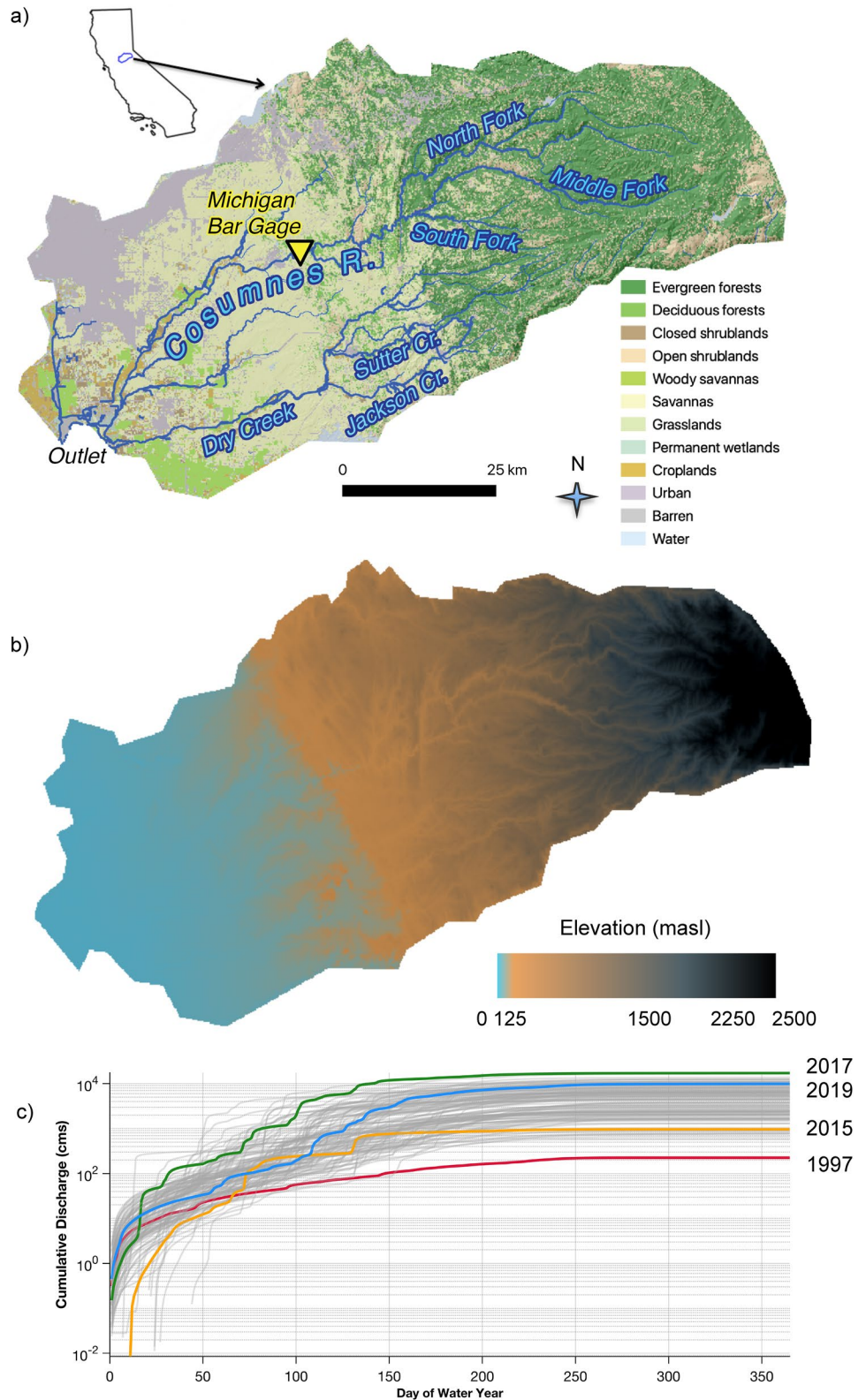


**Figure 1.** (a) Relative location and size of the Cosumnes watershed in California along with the land use and land cover distribution and (b) elevation distribution across the Sacramento Central Valley (blue) and Sierra Nevada (gray to black). (c) Observed streamflow of the Cosumnes river mainstem (at the unimpaired Michigan Bar USGS gage, number 11335000). Water year 2017 (WY2017) had the highest cumulative flow in the >100 years record (green). For reference, other recent extreme years 2019 (blue; wet), 2015 (orange; dry), and 1977 (red; lowest on record) are also shown.



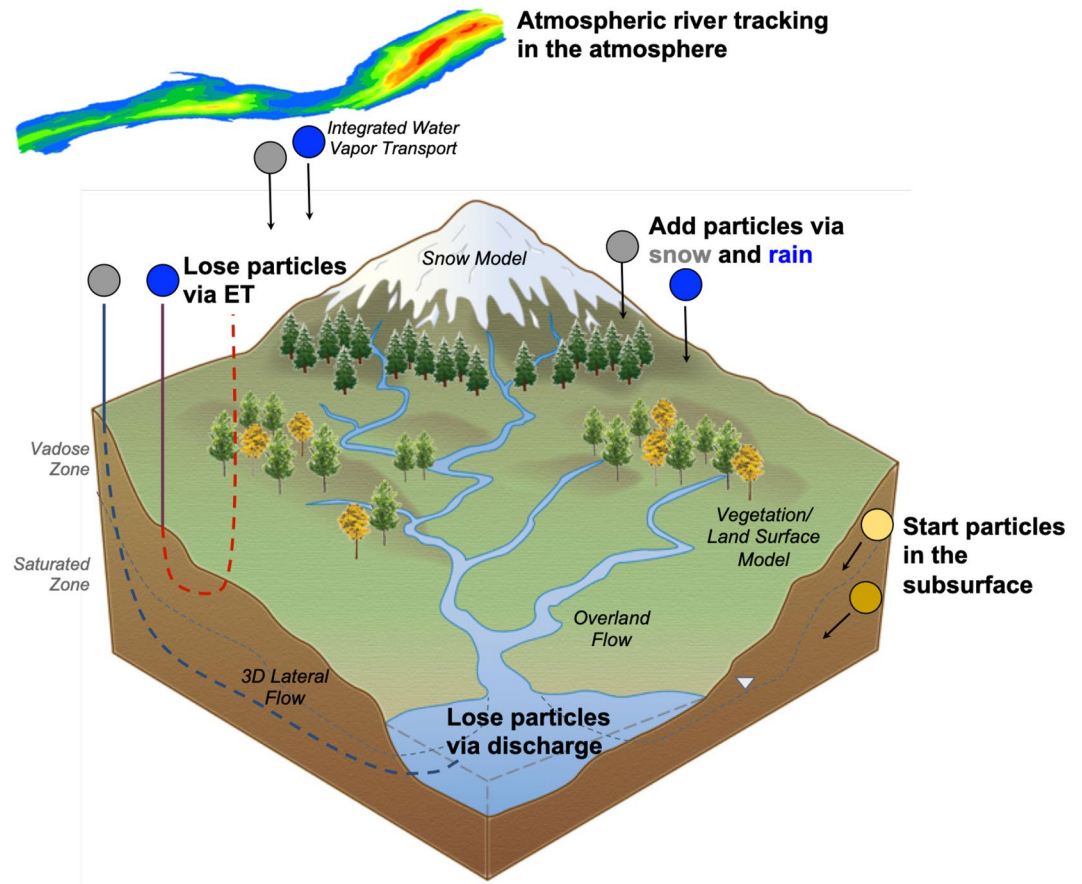


**Figure 2.** Conceptual image of the coupled atmosphere feature tracking scheme used to identify atmospheric rivers (ARs) and connection to subsurface particle tracking, including main processes considered.

TempestExtremes is used to track landfalling ARs during WY17 in the outermost (d01) domain of the WRF simulations (Ullrich & Zarzycki, 2017; Ullrich et al., 2021). To track the ARs we calculate IVT at hourly resolution using meridional and zonal wind speeds and specific humidity across all 30 vertical levels. The AR tracking parameter settings, specifically SplineARs in TempestExtremes, are customized to the spatiotemporal resolution of the WRF simulations (informed by prior research in Rhoades, Jones, O’Brien et al., 2020; Rhoades, Jones, Srivastava, et al., 2020; Rhoades et al., 2021). Parameter settings for TempestExtremes are described in Table 1.

### 3.2. Integrated Hydrologic Flow and Particle Tracking

The integrated hydrologic model ParFlow coupled to the land surface model the Common Land Model (CLM) is used here to simulate the continuum of hydrologic conditions of a representative hillslope spanning from bedrock

**Table 1**  
*TempestExtremes Parameterization Used in This Study*

Parameter	Variable name	Value
Minimum threshold of IVT to be considered an AR	min_val	250 kg/m/s
Minimum Laplacian of IVT	min_laplacian	200,000 kg/m/s/degrees <sup>2</sup>
Minimum area of IVT to be classified as an AR	min_area	68 grid cells
Radius of the discrete Laplacian	size_laplacian	15 grid cells
AR masking via StitchBlobs	–	At least 24 hr and 35 grid cells

*Note.* AR, atmospheric river; IVT, integrated vapor transport.

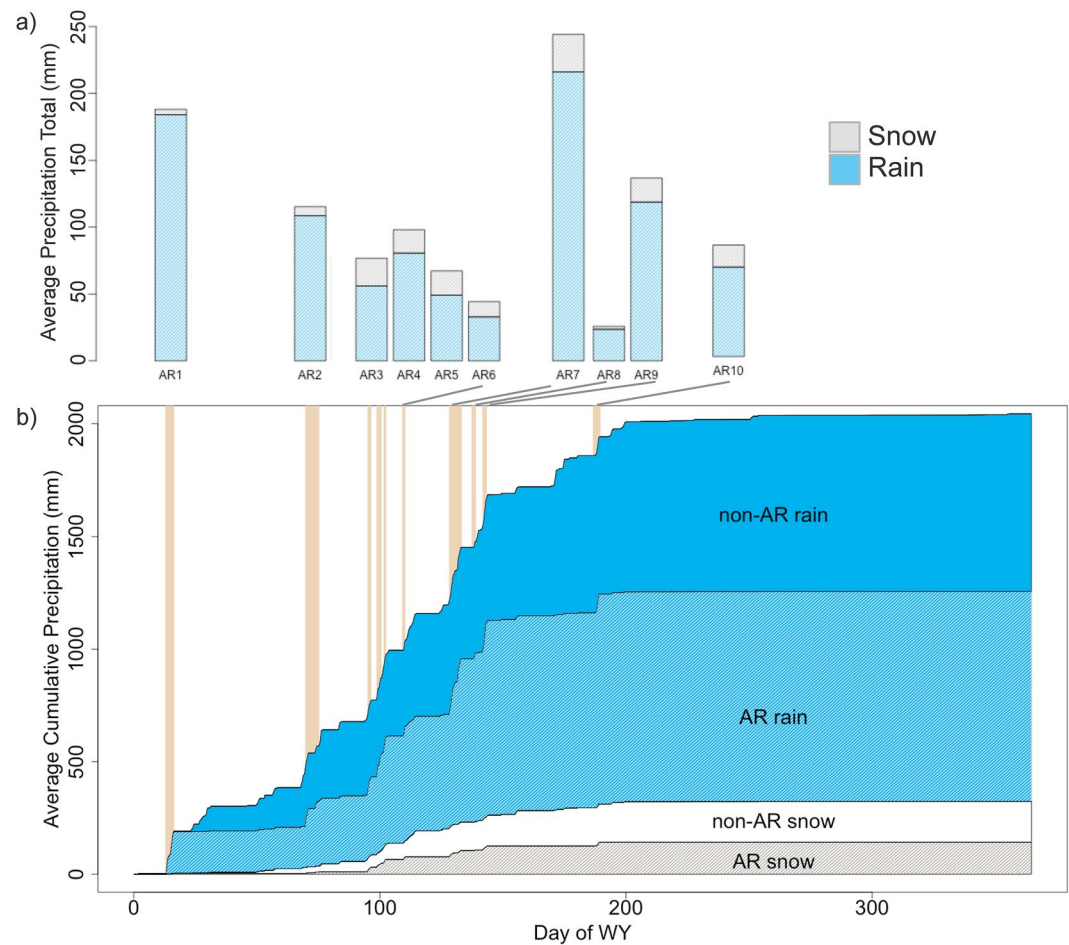


**Figure 3.** (a) Average precipitation total of 10 atmospheric river (AR) events identified by the TempestExtremes tracking algorithm during WY2017 and (b) corresponding watershed-average cumulative precipitation. Periods of AR conditions identified by TempestExtreme are marked by vertical brown boxes. Precipitation is partitioned into rain (blue) and snow (gray and white).

to the lower atmosphere. ParFlow simulates variably saturated and fully saturated flow in three dimensions via the Richards' equation (Richards, 1931) and overland flow in two dimensions via the kinematic wave equation (Ashby & Falgout, 1996; Jones & Woodward, 2001; Kollet & Maxwell, 2006, 2008; Maxwell & Miller, 2005). CLM simulates a coupled water energy balance at the surface layer of the domain by incorporating spatially distributed vegetative processes across specified land use types (Dai et al., 2003). CLM also includes a sophisticated, multi-layer snow model (which includes thermal processes, canopy interception/throughfall, sublimation, snowpack metamorphism and compaction, albedo decay, melt, and snow age) and is further described in detail by Ryken et al. (2020). Land cover is based on the 2011 NLCD Land Use and Land Cover database and is parameterized by the International Geosphere-Biosphere Program (IGBP) database (Homer et al., 2015; International Geosphere, Biosphere Programme, n.d.). Figure 1a shows the distribution of land use and land cover in the Cosumnes watershed; Figure 1b shows the elevation distribution and topography, spanning from the headwaters in the Sierra Nevada to sea level in the Sacramento Central Valley.

The coupled system is forced by eight meteorological variables at an hourly temporal resolution: downwelling long- and short-wave radiation, precipitation, 2-m surface air temperature, 2-m east-to-west (zonal) and north-to-south (meridional) surface winds, atmospheric pressure, and specific humidity, which are supplied via a one-way coupling with the WRF output (Section 3.1). A complete description of the Cosumnes ParFlow-CLM configuration, including input datasets and validation with observations and other remotely sensed datasets can be found in Maina, Siirila-Woodburn, Newcomer, et al. (2020). The spin-up condition to obtain the initial condition, which consists of a one-time spatial kriging to obtain a map of initial pressure field then a simulation period

of precipitation minus evapotranspiration of average climate forcing, then followed by a final step of recursively running a nearly average transient water year (WY2019) recursively until convergence is reached within 1%, similar to Maina et al. (2021) and Maina, Siirila-Woodburn, Newcomer, et al. (2020).

The Lagrangian particle tracking model EcoSLIM is applied to track water particles starting from infiltration at the land surface. For this application, we tag particles as AR or non-AR precipitation based on the feature tracking done by TempestExtremes (see Section 3.1). EcoSLIM uses spatially distributed output from hydrologic models and forcing fields to insert, remove, and move particles (representative of parcels of water) through the flow domain (Maxwell et al., 2019). Evapotranspiration fluxes, subsurface pressure, subsurface saturation, and the three-dimensional subsurface flow velocity fields are provided by ParFlow-CLM. However, the approach used here is fully compatible with other integrated hydrologic models. Particles are introduced into the system via precipitation fluxes (either snow or rain) or initialized as groundwater. Particle mass is determined based on whether the particle was inserted following a precipitation event or initialized as groundwater; all particles are mass weighted. A full description of the code can be found in Maxwell et al. (2019). The model tracks the water source (i.e., snow, rain, or groundwater) of particles moving within the domain and how they exit the domain through either evapotranspiration or outflow. Corresponding residence times of all particles are also quantified, relying on an optimal local time-step of particle movement based on a prior version of the SLIM and SLIM-FAST codes (Maxwell, 2010) used previously to simulate an array of subsurface flow dynamics (Bearup et al., 2016; Moqbel & Abu-El-Sha'r, 2018; Siirila & Maxwell, 2012; Siirila et al., 2012; Siirila-Woodburn, Fernández-García, & Sanchez-Vila, 2015; Siirila-Woodburn & Maxwell, 2015; Siirila-Woodburn, Sanchez-Vila, & Fernández-García, 2015). The Ito-Fokker-Planck approximation is used to simulate the advection-dispersion equation (see Maxwell et al., 2007 for full formulation). Velocity interpolation is linear following Danesh-Yazdi et al. (2018).

The spin-up procedure for the particle tracking model follows after that of the ParFlow-CLM spin-up, and consists of initializing one particle per cell starting with the pressure head distribution based on the final condition of ParFlow-CLM spin-up. The EcoSLIM spin-up begins with the final step of the ParFlow-CLM spin-up by recursively running the nearly average transient WY2019 until convergence has been reached, in this case around 35 years of simulation time. This ensures that both the velocity field (from ParFlow-CLM) and residence time distribution of the particles (from EcoSLIM) are converged. Following the spin-up, we then compare the evolution of particle mass that exit or remain in groundwater storage during WY2017, partitioned by water source (i.e., rain, snow, or groundwater). Storage of each cell either saturated ( $\text{Storage}_{\text{Sat}}$ ) or unsaturated ( $\text{Storage}_{\text{Unsat}}$ ), is calculated as follows:

$$\text{Storage}_{\text{Unsat}} = (\text{Sat} * \phi * dx * dy * dz) \quad (1a)$$

$$\text{Storage}_{\text{Sat}} = (\text{Sat} * \psi * SS * dx * dy * dz) + (\text{Sat} * \phi * dx * dy * dz) \quad (1b)$$

where  $\phi$  is the cell porosity (–),  $dx$ ,  $dy$ ,  $dz$  are respectively the  $x$ -,  $y$ -, and  $z$ -cell resolutions (–),  $\psi$  is the cell pressure head (m), and  $SS$  is the specific storage ( $\text{m}^{-1}$ ).

RoS events are identified when precipitation falls in the form of rain over cells that have snow water equivalent (SWE) greater than zero; any infiltrating particles over these regions are tracked in EcoSLIM as snow and further classified/tracked as RoS particles. As with all the dynamically added subsurface particles within EcoSLIM, the amount of RoS subsurface particles is determined by the net infiltration at the land surface, so that RoS particles are the result of the water-energy balance within the snowpack resulting in snowmelt, and not the precipitation rate alone.

## 4. Results and Discussion

### 4.1. AR Identification and Rain-Snow Partitioning

The cumulative precipitation total of WY2017, as well as the water partitioning between snow and rain, and AR events as identified via Tempest Extremes, and non-AR events, which is any other precipitation outside the identified AR windows, are shown in Figure 3. The majority of large precipitation events corresponding to sharp steps in the cumulative precipitation time series are identified as ARs (brown vertical boxes), although some exceptions exist. For example, note a precipitation event around WY day 180. WY2017 precipitation totals indicate that 52% of precipitation is provided by ARs. The majority of both AR and non-AR precipitation is in the form of rain and ARs contribute less snowfall than non-ARs: 19% of non-AR precipitation falls as snow, whereas only 13% of AR precipitation is snowfall. Across the 10 storms, all produce a mixture of snow and rain. We reserve any inferences



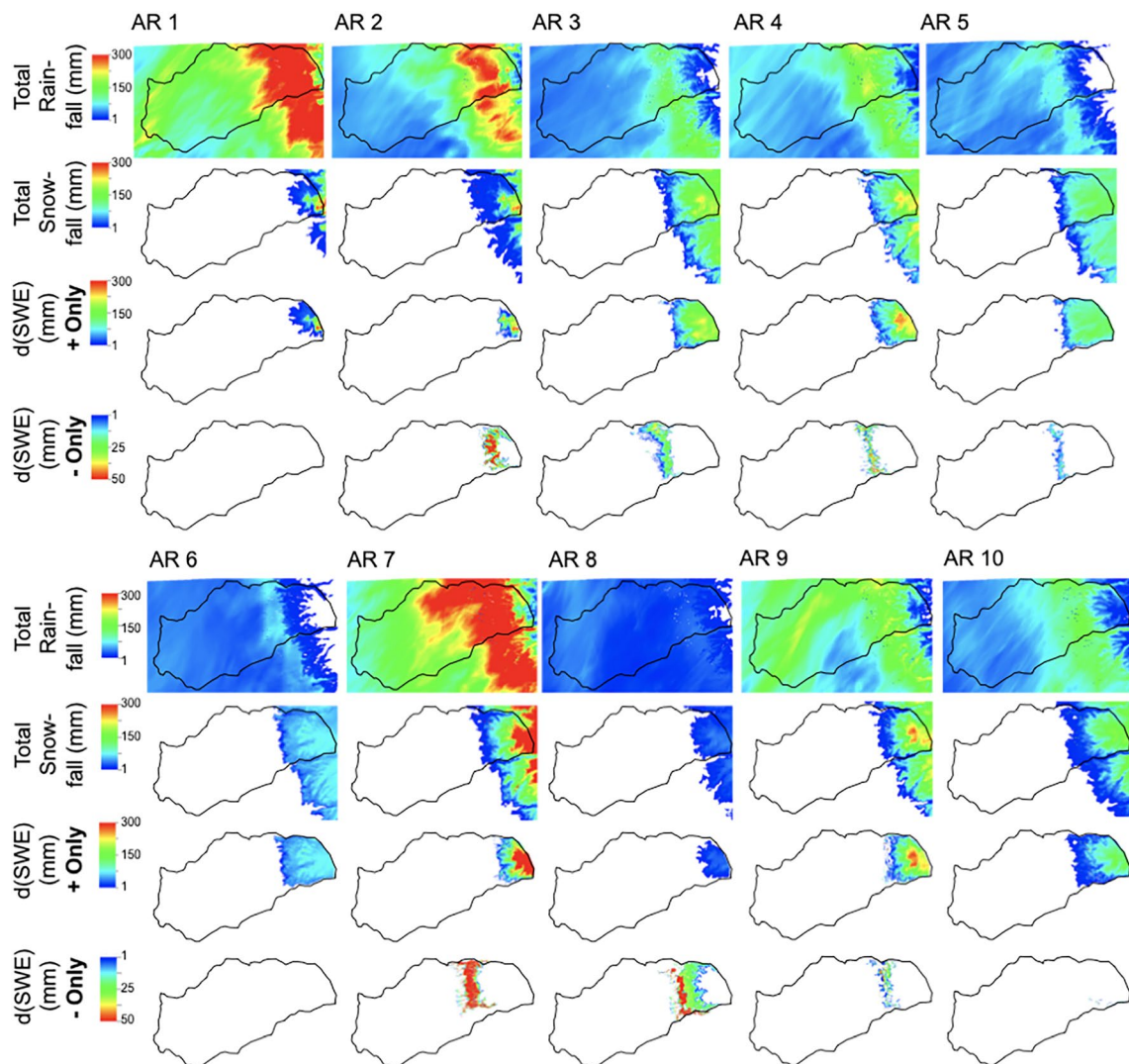


**Figure 4.** Spatial distribution of total rainfall, snowfall, and post-storm changes in snow water equivalent (SWE) across the 10 atmospheric rivers (ARs) identified in WY2017.

about temporal trends with magnitude, rain-snow-partitioning, etc., given the storm sample size; however, an examination of storm-by-storm behavior is helpful to understand system dynamics.

#### 4.2. Individual AR Characteristics and Impacts on Snowpack

Simulated maps of the AR-specific total rainfall and snowfall show an orographic dependence with greater precipitation occurring at higher elevations, in the headwaters of the Sierra Nevada (Figure 4). In the highest elevations of the watershed (1,500–2,500 m), all of the storms produce snowfall, and most (7 of 10) ARs produce a mixture of rainfall and snowfall over the duration of the storm. All ARs result in an increase in SWE in the headwaters, in some regions in excess of 300 mm during a single storm. Most of the ARs also result in RoS at intermediate elevations (between approximately 500–1,500 m), resulting in a clear elevation band of decreases in SWE. Of the 10 ARs, the only storms that do not result in a decrease in SWE are those that have negligible or nonexistent snowpacks prior to the onset of the storm (AR 1 and AR 10), and one smaller storm, which was also colder (AR 6).

#### 4.3. Hydrologic Water Partitioning and Contributions to Groundwater

A basin-wide water budget partition of WY2017 precipitation is shown in Figure 5. The year-end fate of WY2017 precipitation is partitioned as either exited particles (evapotranspiration,  $ET$ , or discharge,  $Q$ ), or into groundwater

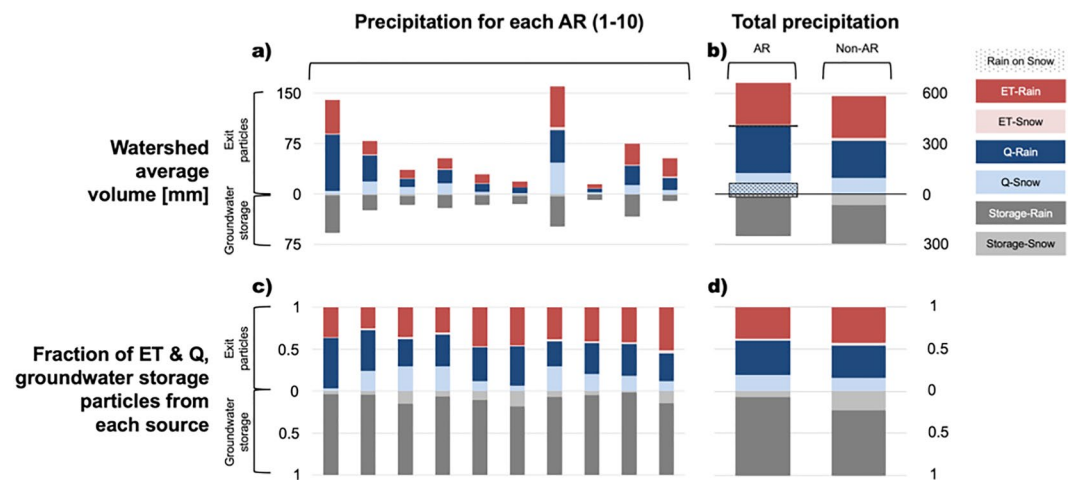


**Figure 5.** Water partitioning for (a) the 10 identified atmospheric rivers (ARs), and (b) annual totals of ARs compared to non-AR precipitation. Precipitation-normalized values are shown in (c) and (d), respectively.

storage (both for individual storms and for water year totals; Figure 5). A time-series of basin-wide water partitioning is included in Figure S1 in Supporting Information S1. Despite ARs contributing 52% of the annual precipitation, AR precipitation results in 15% less water going to annual groundwater storage than non-ARs (Figure 3b). In part, this difference can be attributed to the characteristically high rainfall rates of ARs and therefore greater potential for less infiltration and more runoff (either via infiltration excess overland flow or, if the storm duration is sufficient enough and/or the antecedent soil moisture conditions were wet enough, via saturation excess). Because ParFlow-CLM allows for both saturation excess and infiltration excess to be simulated, both runoff generation types are considered here. Interestingly, 93% of the AR contribution to groundwater is derived from rain, whereas groundwater contributions from non-ARs are 77% from rain and 23% from snow. Recall that annual snowfall amounts from ARs and non-AR storms are nearly equivalent (see Figure 3), so the differences in groundwater composition (rain vs. snow derived) cannot be attributed to snowfall-derived precipitation amounts. A possible explanation for the difference in groundwater contribution source is the high prevalence of RoS conditions during ARs (see Section 4.2). Figure 5b also shows the fraction of each water compartment that was derived from RoS events (stippled boxes). RoS largely governs discharge resulting from AR precipitation, where over half of discharge stems from AR-driven RoS events. In contrast, a negligible amount of non-AR discharge is driven by RoS events.

The fractional behavior of the 10 ARs (Figure 5c) and annual totals (Figure 5d) help to differentiate and quantify contributions more explicitly when the volumes are normalized by precipitation amount. Fractionally, the behavior of AR and non-AR precipitation are very similar (Figure 5d), *except* for the contributions to groundwater from rain versus snow. Importantly, AR snow contributes significantly less to groundwater compared to non-AR snow: approximately 300% more non-AR snow resides in groundwater storage by year end compared to AR snow. These results suggest that the most significant difference in AR-sourced precipitation is on the groundwater recharge-snow relationship.

#### 4.4. Dynamic Groundwater Storage

To better understand groundwater dynamics through WY2017 and between the vadose and saturated zone, Figure 6 shows the hourly relationship between watershed-averaged saturated and unsaturated storage, color-coded by month in (a) and by individual storm in (b). The cross-hairs of each diagram indicate the initial state of the storage at 1 October 2016, and the four quadrants indicate relative increases/decreases relative to that point in time. By plotting the dynamic interaction of saturated and unsaturated storage, we are able to better understand overall groundwater storage in the presence (and absence) of ARs, as well as the system response through time. AR event-based (Figure S2 in Supporting Information S1) and monthly (Figure S3 in Supporting Information S1) groundwater pressure head change maps are included in Supporting Information S1.

October groundwater storage (Figure 6a) shows the continued decline of the overall storage during the tail-end of summer baseflow conditions, but is quickly followed by sharp increases in winter and spring storage where

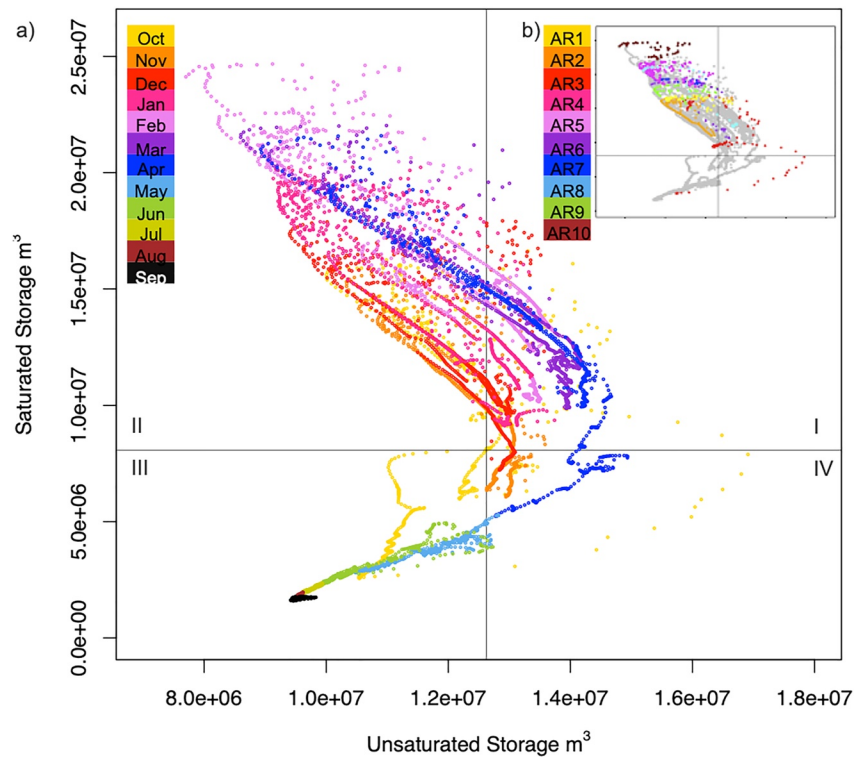


**Figure 6.** Relationship between saturated and unsaturated groundwater storage through time. Occurrence in the four quadrants (I–IV) describes how groundwater storage changes relative to the initial state of WY2017 (cross-hairs). Hourly trends are grouped by monthly color-coding in (a) and by the 10 atmospheric rivers (ARs) in (b).

the majority of storage variation occurs. During these wet months, relatively high groundwater storage increases from the initial state are evident. The timing of the 10 discrete AR events (Figure 6b; note separate color-legend) shows sharp and rapid changes in groundwater dynamics during two periods. These include periods when both the saturated and unsaturated storage are larger than the initial states (quadrant I), but also during long periods of higher saturated storage and lower unsaturated storage relative to the initial state (quadrant II). The latter occurs as near-surface variably saturated regions become completely saturated, effectively acting as a “trade-off” of storage as that residual storage becomes saturated. Lastly, as the final spring precipitation events occur and snow melts in April, the dynamic storage trend down toward quadrant III, where both saturated and unsaturated groundwater storage show decline relative to initial groundwater states. These simulations suggest that total groundwater storage will decrease by year-end relative to the beginning of the WY, despite WY2017 being the wettest on record for the Cosumnes watershed. This is consistent with Maina, Siirila-Woodburn, Newcomer, et al. (2020), which showed that groundwater pumping rates in the Sacramento Central Valley result in a net negative impact on watershed-average groundwater storage even during WY2017.

## 5. Conclusions

ARs play a central role in western United States precipitation, but to date there exists a lack of knowledge on how these storms impact the integrated hydrologic cycle, especially groundwater, which is crucial to long-term water resources and especially during periods of drought. With the use of coupled, atmosphere and integrated hydrologic models and above-, and below-ground water tracking techniques, we simulate a record wet year of an unimpaired northern California watershed. We used this model to draw lessons learned from how AR and non-AR water partitioning drives groundwater recharge. To the best of our knowledge, this study is the first to examine the role in which ARs contribute to groundwater dynamics. Our primary results include:

1. Despite ARs contributing over half of annual total precipitation, the contribution to end-of-year groundwater storage is less than the contribution made by non-AR precipitation.

2. Occurrences of RoS plays an important role in AR-driven discharge, where over half of AR discharge from snow comes from RoS events.
3. ARs result in 300% less snow-derived groundwater-recharge compared to non-ARs.
4. Despite WY2017 being the wettest year on record, groundwater pumping results in a net loss of groundwater storage by year-end.

Computational limitations associated with the full atmosphere-through-bedrock modeling and tracking algorithms, both which required supercomputing resources, limited the period of examination (a single water year; albeit an extreme year) that we could conduct in this study. Thus, our study represents a “proof of concept” for future work when computing resources enable us to conduct a longer set of simulations that better estimate the range of climate variability in California. WY2017 provides, at least, a partial analogue into the future given the higher occurrence and intensity of ARs that occurred. Antecedent soil moisture and groundwater conditions prior to each storm may impact the hydrologic response of each storm, especially the first storm of the season following a dry summer; here we focus on the hydrologic response of an observed extremely wet winter with a large sample size of ARs to understand their individually sequenced, and aggregate response on the hydrologic cycle to develop some key “lessons learned.” Future studies could expand this study design to consider more scenarios of AR impacts on hydrology such as drought years with occasional extreme ARs (e.g., WY2015 or WY2018) or more near-average years (e.g., WY2009 or WY2016). Future studies could also consider the process-based hydrologic changes of ARs we have examined here but in conjunction with their societal and environmental impacts such as flooding (e.g., Konrad & Dettinger, 2017), levee breaks (e.g., Florsheim & Dettinger, 2015), and postfire debris flows (e.g., Oakley et al., 2017).

The results presented here suggest serious implications for groundwater recharge and water management given a future where annual precipitation is derived from larger, more intense, and warmer storms. Future studies may also examine AR conditions such as those from WY2017 but with synthetic modifications such as warmer air temperatures, different water demands and/or antecedent conditions, changes in precipitation phase (i.e., a low-to-no snow future; Siirila-Woodburn et al., 2021), and with changes in vegetation and/or land use (as projected by Earth system models in the coming decades) or different spring season characteristics (e.g., McEvoy & Hatchett, 2023). Isolating these factors of future climate conditions in the presence of ARs may help to inform watershed dynamics in the future as well as prioritizing investments intended to minimize flood risk and maximize water storage, including flood protection measures for unimpaired basins, water capture and recharge procedures such as managed aquifer recharge, and in basins with reservoirs, optimization of surface water reservoir and conveyance operations such as forecast informed reservoir operations.

#### Acknowledgments

This research used computing resources from the National Energy Research Scientific Computing Center, a DOE Office of Science User Facility supported by the US Department of Energy (contract no. DE-AC02-05CH11231). Siirila-Woodburn, Dennedy-Frank, and Maina were supported by funding from Berkeley Lab, provided by the Director, Office of Science, of the U.S. Department of Energy under Contract DE-AC02-05CH11231. Rhoades, Vahmani, and Zhou were funded by the Director, Office of Science, Office of Biological and Environmental Research of the U.S. Department of Energy Regional and Global Climate Modeling Program (RGCM) “the Calibrated and Systematic Characterization, Attribution and Detection of Extremes (CASCADE)” Science Focus Area (award no. DE-AC02-05CH11231). Jones and Rhoades were funded by the Director, Office of Science, Office of Biological and Environmental Research of the U.S. Department of Energy Regional and Global Climate Modeling Program (RGCM) “An Integrated Evaluation of the Simulated Hydroclimate System of the Continental US” project (award no. DE-SC0016605). Hatchett was funded by the Sulo and Aileen Maki Endowment.

#### Data Availability Statement

Model simulations were performed with the following open source codes: WRF version 3.6.1 available at <https://github.com/wrf-model/WRF>, TempestExtremes version 1 available at <https://github.com/ClimateGlobalChange/tempestextremes>, ParFlow-CLM version 3.9.0 available at <https://github.com/parflow>, and EcoSLIM version 1.3 available at <https://github.com/reedmaxwell/EcoSLIM>. Archiving for TempestExtremes data used in this study is available via Science Gateways at [https://portal.nersc.gov/archive/home/a/rhoades/Shared/www/WRR\\_2020](https://portal.nersc.gov/archive/home/a/rhoades/Shared/www/WRR_2020) (Rhoades, 2023). Archiving for WRF, ParFlow-CLM, and EcoSLIM modeling data used in this study is available at Zenodo via <https://doi.org/10.5281/zenodo.7545440> (Siirila-Woodburn, 2023) and <https://github.com/erwoodburn/Siirila-Woodburn-et-al.-WRR-2023.git> (Siirila-Woodburn, 2023).

#### References

- Ashby, S. F., & Falgout, R. D. (1996). A parallel multigrid preconditioned conjugate gradient algorithm for groundwater flow simulations. *Nuclear Science and Engineering: The Journal of the American Nuclear Society*, 124(1), 145–159. <https://doi.org/10.13182/NSE96-A24230>
- Bearup, L. A., Maxwell, R. M., & McCray, J. E. (2016). Hillslope response to insect-induced land-cover change: An integrated model of end-member mixing: Modelling the hillslope mixing response to land-cover change. *Ecology*, 97(2), 195–203. <https://doi.org/10.1002/eoc.1729>
- Bretherton, C. S., & Park, S. (2009). A new moist turbulence parameterization in the Community Atmosphere Model. *Journal of Climate*, 22(12), 3422–3448. <https://doi.org/10.1175/2008jcli2556.1>
- Chen, X., Leung, L. R., Wigmosta, M., & Richmond, M. (2019). Impact of atmospheric rivers on surface hydrological processes in western U.S. watersheds. *Journal of Geophysical Research*, 124(16), 8896–8916. <https://doi.org/10.1029/2019jd030468>
- Dai, X. P., Xeng, X., Dickinson, R. E., Baker, I., Bonan, G. B., Bosilovich, M. G., et al. (2003). The Common Land Model. *Bulletin of the American Meteorological Society*, 84(8), 1013–1024. <https://doi.org/10.1175/BAMS-84-8-1013>



- Danesh-Yazdi, M., Klaus, J., Condon, L. E., & Maxwell, R. M. (2018). Bridging the gap between numerical solutions of travel time distributions and analytical storage selection functions. *Hydrological Processes*, 32(8), 1063–1076. <https://doi.org/10.1002/hyp.11481>
- de Rooij, R., Graham, W., & Maxwell, R. M. (2013). A particle-tracking scheme for simulating pathlines in coupled surface-subsurface flows. *Advances in Water Resources*, 52, 7–18. <https://doi.org/10.1016/j.advwatres.2012.07.022>
- Dettinger, M. D., Ralph, F. M., Das, T., Neiman, P. J., & Cayan, D. R. (2011). Atmospheric rivers, floods and the water resources of California. *Water*, 3(2), 445–478. <https://doi.org/10.3390/w3020445>
- Dudhia, J. (1989). Numerical study of convection observed during the winter monsoon experiment using a mesoscale two-dimensional model. *Journal of the Atmospheric Sciences*, 46(20), 3077–3107. [https://doi.org/10.1175/1520-0469\(1989\)046<3077:nsocod>2.0.co;2](https://doi.org/10.1175/1520-0469(1989)046<3077:nsocod>2.0.co;2)
- Earman, S., Campbell, A. R., Phillips, F. M., & Newman, B. D. (2006). Isotopic exchange between snow and atmospheric water vapor: Estimation of the snowmelt component of groundwater recharge in the southwestern United States. *Journal of Geophysical Research*, 111(D9), D09302. <https://doi.org/10.1029/2005jd006470>
- Famiglietti, J. S. (2014). The global groundwater crisis. *Nature Climate Change*, 4(11), 945–948. <https://doi.org/10.1038/nclimate2425>
- Florsheim, J., & Dettinger, M. (2015). Promoting atmospheric-river and snowmelt-fueled biogeomorphic processes by restoring river-floodplain connectivity in California's Central Valley. In P. Hudson, & H. Middelkoop (Eds.), *Geomorphic approaches to integrated floodplain management of lowland fluvial systems in North America and Europe* (pp. 119–141). Springer. [https://doi.org/10.1007/978-1-4939-2380-9\\_6](https://doi.org/10.1007/978-1-4939-2380-9_6)
- Gao, Y., Lu, J., Leung, L. R., Yang, Q., Hagos, S., & Qian, Y. (2015). Dynamical and thermodynamical modulations on future changes of landfalling atmospheric rivers over Western North America. *Geophysical Research Letters*, 42(17), 7179–7186. <https://doi.org/10.1002/2015GL065435>
- Gershunov, A., Shulgina, T., Clemesha, R. E. S., Guirguis, K., Pierce, D. W., Dettinger, M. D., et al. (2019). Precipitation regime change in western North America: The role of atmospheric rivers. *Scientific Reports*, 9(1), 9944. <https://doi.org/10.1038/s41598-019-46169-w>
- Gershunov, A., Shulgina, T., Ralph, F. M., Lavers, D. A., & Rutz, J. J. (2017). Assessing the climate-scale variability of atmospheric rivers affecting western North America. *Geophysical Research Letters*, 44(15), 7900–7908. <https://doi.org/10.1002/2017gl074175>
- Grell, G. A., & Freitas, S. R. (2014). A scale and aerosol aware stochastic convective parameterization for weather and air quality modeling. *Atmospheric Chemistry and Physics*, 14(10), 5233–5250. <https://doi.org/10.5194/acp-14-5233-2014>
- Guan, B., Waliser, D. E., Ralph, F. M., Fetzer, E. J., & Neiman, P. J. (2016). Hydrometeorological characteristics of rain-on-snow events associated with atmospheric rivers. *Geophysical Research Letters*, 43(6), 2964–2973. <https://doi.org/10.1002/2016GL067978>
- Haleakala, K., Brandt, W. T., Hatchett, B. J., Li, D., Lettenmaier, D. P., & Gebremichael, M. (2022). Watershed memory amplified the Oroville rain-on-snow flood of February 2017. *PNAS Nexus*, 2022, pgac295. <https://doi.org/10.1093/pnasnexus/pgac295>
- Hatchett, B. J., Daudert, B., Garner, C. B., Oakley, N. S., Putnam, A. E., & White, A. B. (2017). Winter snow level rise in the northern Sierra Nevada from 2008 to 2017. *Water*, 9(11), 899. <https://doi.org/10.3390/w9110899>
- Homer, C., Dewitz, J., Yang, L., Jin, S., Danielson, P., Xian, G., et al. (2015). Completion of the 2011 National Land Cover Database for the conterminous United States—Representing a decade of land cover change information. *Photogrammetric Engineering & Remote Sensing*, 81(5), 346–354. <https://doi.org/10.14358/PERS.81.5.345>
- Hu, H., Dominguez, F., Kumar, P., McDonnell, J., & Gochis, D. (2018). A numerical water tracer model for understanding event-scale hydrometeorological phenomena. *Journal of Hydrometeorology*, 19(6), 947–967. <https://doi.org/10.1175/JHM-D-17-0202.1>
- Inda-Díaz, H. A., O'Brien, T. A., Zhou, Y., & Collins, W. D. (2021). Constraining and characterizing the size of atmospheric rivers: A perspective independent from the detection algorithm. *Journal of Geophysical Research*, 126(16), e2020JD033746. <https://doi.org/10.1029/2020jd033746>
- International Geosphere-Biosphere Programme. (n.d.). Retrieved from <http://www.igbp.net/>
- Jones, J. E., & Woodward, C. S. (2001). Newton–Krylov-multigrid solvers for large-scale, highly heterogeneous, variably saturated flow problems. *Advances in Water Resources*, 24(7), 763–774. [https://doi.org/10.1016/S0309-1708\(00\)00075-0](https://doi.org/10.1016/S0309-1708(00)00075-0)
- Kollet, S. J., & Maxwell, R. M. (2006). Integrated surface–groundwater flow modeling: A free-surface overland flow boundary condition in a parallel groundwater flow model. *Advances in Water Resources*, 29(7), 945–958. <https://doi.org/10.1016/j.advwatres.2005.08.006>
- Kollet, S. J., & Maxwell, R. M. (2008). Capturing the influence of groundwater dynamics on land surface processes using an integrated, distributed watershed model. *Water Resources Research*, 44(2). <https://doi.org/10.1029/2007wr006004>
- Konrad, C. P., & Dettinger, M. D. (2017). Flood runoff in relation to water vapor transport by atmospheric rivers over the western United States, 1949–2015. *Geophysical Research Letters*, 44(22), 11456–11462. <https://doi.org/10.1002/2017gl075399>
- Lavers, D. A., & Villarini, G. (2015). The contribution of atmospheric rivers to precipitation in Europe and the United States. *Journal of Hydrology*, 522, 382–390. <https://doi.org/10.1016/j.jhydrol.2014.12.010>
- Maina, F. Z., Rhoades, A., Siirila-Woodburn, E. R., & Dennedy-Frank, P.-J. (2021). Projecting the impacts of end of century climate extremes on the hydrology in California. *Hydrology and Earth System Sciences: Discussions*. <https://doi.org/10.5194/hess-2021-472>
- Maina, F. Z., & Siirila-Woodburn, E. R. (2019). Watersheds dynamics following wildfires: Nonlinear feedbacks and implications on hydrologic responses. *Hydrological Processes*, 34(1), 33–50. <https://doi.org/10.1002/hyp.13568>
- Maina, F. Z., Siirila-Woodburn, E. R., Newcomer, M., Xu, Z., & Steefel, C. (2020). Determining the impact of a severe dry to wet transition on watershed hydrodynamics in California, USA with an integrated hydrologic model. *Journal of Hydrology*, 580, 124358. <https://doi.org/10.1016/j.jhydrol.2019.124358>
- Maina, F. Z., Siirila-Woodburn, E. R., & Vahmani, P. (2020). Sensitivity of meteorological-forcing resolution on hydrologic variables. *Hydrology and Earth System Sciences*, 24(7), 3451–3474. <https://doi.org/10.5194/hess-24-3451-2020>
- Maxwell, R. M. (2010). SLIM-FAST: A user's manual V.4. *GWMI 2010*, 1, 49.
- Maxwell, R. M., Condon, L. E., Danesh-Yazdi, M., & Bearup, L. A. (2019). Exploring source water mixing and transient residence time distributions of outflow and evapotranspiration with an integrated hydrologic model and Lagrangian particle tracking approach: Source water mixing and transient residence time distributions ET and Q. *Ecohydrology*, 12(1), e2042. <https://doi.org/10.1002/eco.2042>
- Maxwell, R. M., & Miller, N. L. (2005). Development of a coupled land surface and groundwater model. *Journal of Hydrometeorology*, 6(3), 233–247. <https://doi.org/10.1175/JHM422.1>
- Maxwell, R. M., Welty, C., & Harvey, R. W. (2007). Revisiting the Cape Cod bacteria injection experiment using a stochastic modeling approach. *Environmental Science & Technology*, 41(15), 5548–5558. <https://doi.org/10.1021/es062693a>
- McEvoy, D., & Hatchett, B. J. (2023). Spring heat waves drive record western United States snow melt in 2021. *Environmental Research Letters*, 18(1), 014007. <https://doi.org/10.1088/1748-9326/aca8bd>
- Meixner, T., Manning, A. H., Stonestrom, D. A., Allen, D. M., Ajami, H., Blasch, K. W., et al. (2016). Implications of projected climate change for groundwater recharge in the western United States. *Journal of Hydrology*, 534, 124–138. <https://doi.org/10.1016/j.jhydrol.2015.12.027>
- Michaelis, A. C., Gershunov, A., Weyant, A., Fish, M. A., Shulgina, T., & Ralph, F. M. (2022). Atmospheric river precipitation enhanced by climate change: A case study of the storm that contributed to California's Oroville Dam crisis. *Earth's Future*, 10(3), e2021EF002537. <https://doi.org/10.1029/2021EF002537>

- Mlawer, E. J., Taubman, S. J., Brown, P. D., Iacono, M. J., & Clough, S. A. (1997). Radiative transfer for inhomogeneous atmospheres: RRTM, a validated correlated-k model for the longwave. *Journal of Geophysical Research*, *102*(D14), 16663–16682. <https://doi.org/10.1029/97jd00237>
- Monin, A. S., & Obukhov, A. M. (1954). Basic laws of turbulent mixing in the surface layer of the atmosphere. *Contributions of the Geophysical Institute of the Slovak Academy of Sciences*, *151*, 163–187. (in Russian).
- Moqbel, S., & Abu-El-Sha'r, W. (2018). Modeling groundwater flow and solute transport at Azraq basin using ParFlow and Slim-Fast. *Jordan Journal of Civil Engineering; Irbid*, *12*(2). Retrieved from <https://search.proquest.com/scholarly-journals/modeling-groundwater-flow-solute-transport-at/docview/2033016065/se-2>
- Morrison, H., Thompson, G., & Tatarskii, V. (2009). Impact of cloud microphysics on the development of trailing stratiform precipitation in a simulated squall line: Comparison of one- and two-moment schemes. *Monthly Weather Review*, *137*(3), 991–1007. <https://doi.org/10.1175/2008mwr2556.1>
- Neiman, P. J., Martin Ralph, F., Wick, G. A., Lundquist, J. D., & Dettinger, M. D. (2008). Meteorological characteristics and overland precipitation impacts of atmospheric rivers affecting the west coast of North America based on eight years of SSM/I satellite observations. *Journal of Hydrometeorology*, *9*(1), 22–47. <https://doi.org/10.1175/2007JHM855.1>
- Oakley, N. S., Lancaster, J. T., Kaplan, M. L., & Ralph, F. M. (2017). Synoptic conditions associated with cool season post-fire debris flows in the Transverse Ranges of southern California. *Natural Hazards*, *88*(1), 327–354. <https://doi.org/10.1007/s11069-017-2867-6>
- O'Brien, T. A., Wehner, M. F., Payne, A. E., Shields, C. A., Rutz, J. J., Leung, L.-R., et al. (2022). Increases in future AR count and size: Overview of the ARTMIP tier 2 CMIP5/6 experiment. *Journal of Geophysical Research*, *127*(6). <https://doi.org/10.1029/2021jd036013>
- Patricola, C. M., Wehner, M. F., Bercos-Hickey, E., Maciel, F. V., May, C., Mak, M., et al. (2022). Future changes in extreme precipitation over the San Francisco Bay Area: Dependence on atmospheric river and extratropical cyclone events. *Weather and Climate Extremes*, *36*, 100440. <https://doi.org/10.1016/j.wace.2022.100440>
- Payne, A. E., Demory, M.-E., Ruby Leung, L., Ramos, A. M., Shields, C. A., Rutz, J. J., et al. (2020). Responses and impacts of atmospheric rivers to climate change. *Nature Reviews Earth & Environment*, *1*(3), 143–157. <https://doi.org/10.1038/s43017-020-0030-5>
- Radić, V., Cannon, A. J., Menounos, B., & Gi, N. (2015). Future changes in autumn atmospheric river events in British Columbia, Canada, as projected by CMIP5 global climate models. *Journal of Geophysical Research*, *120*(18), 9279–9302. <https://doi.org/10.1002/2015jd023279>
- Ralph, F. M., Coleman, T., Neiman, P. J., Zamora, R. J., & Dettinger, M. D. (2013). Observed impacts of duration and seasonality of atmospheric-river landfalls on soil moisture and runoff in coastal northern California. *Journal of Hydrometeorology*, *14*(2), 443–459. <https://doi.org/10.1175/JHM-D-12-076.1>
- Ralph, F. M., Dettinger, M., Lavers, D., Gorodetskaya, I. V., Martin, A., Viale, M., et al. (2017). Atmospheric rivers emerge as a global science and applications focus. *Bulletin of the American Meteorological Society*, *98*(9), 1969–1973. <https://doi.org/10.1175/BAMS-D-16-0262.1>
- Ralph, F. M., Iacobellis, S. F., Neiman, P. J., Cordeira, J. M., Spackman, J. R., Waliser, D. E., et al. (2017). Dropsonde observations of total integrated water vapor transport within North Pacific atmospheric rivers. *Journal of Hydrometeorology*, *18*(9), 2577–2596. <https://doi.org/10.1175/JHM-D-17-0036.1>
- Ralph, F. M., Neiman, P. J., Wick, G. A., Gutman, S. I., Dettinger, M. D., Cayan, D. R., & White, A. B. (2006). Flooding on California's Russian River: Role of atmospheric rivers. *Geophysical Research Letters*, *33*(13), L13801. <https://doi.org/10.1029/2006gl026689>
- Rhoades, A. M. (2023). HPSS archive: Listing of /home/a/rhoades/Shared/www/WRR\_2020/. [Dataset]. Science Gateways. Retrieved from [https://portal.nersc.gov/archive/home/a/rhoades/Shared/www/WRR\\_2020](https://portal.nersc.gov/archive/home/a/rhoades/Shared/www/WRR_2020)
- Rhoades, A. M., Jones, A. D., O'Brien, T. A., O'Brien, J. P., Ullrich, P. A., & Zarzycki, C. M. (2020). Influences of North Pacific Ocean domain extent on the western U.S. winter hydroclimatology in variable-resolution CESM. *Journal of Geophysical Research*, *125*(14). <https://doi.org/10.1029/2019jd031977>
- Rhoades, A. M., Jones, A. D., Srivastava, A., Huang, H., O'Brien, T. A., Patricola, C. M., et al. (2020). The shifting scales of western U.S. land-falling atmospheric rivers under climate change. *Geophysical Research Letters*, *47*(17). <https://doi.org/10.1029/2020gl089096>
- Rhoades, A. M., Risser, M. D., Stone, D. A., Wehner, M. F., & Jones, A. D. (2021). Implications of warming on western United States landfalling atmospheric rivers and their flood damages. *Weather and Climate Extremes*, *32*, 100326. <https://doi.org/10.1016/j.wace.2021.100326>
- Richards, L. A. (1931). Capillary conduction of liquids through porous mediums. *Physics*, *1*(5), 318–333. <https://doi.org/10.1063/1.1745010>
- Rutz, J. J., James Steenburgh, W., & Martin Ralph, F. (2014). Climatological characteristics of atmospheric rivers and their inland penetration over the western United States. *Monthly Weather Review*, *142*(2), 905–921. <https://doi.org/10.1175/MWR-D-13-00168.1>
- Rutz, J. J., Shields, C. A., Lora, J. M., Payne, A. E., Guan, B., Ullrich, P., et al. (2019). The Atmospheric River Tracking Method Intercomparison Project (ARTMIP): Quantifying uncertainties in atmospheric river climatology. *Journal of Geophysical Research*, *124*(24), 13777–13802. <https://doi.org/10.1029/2019jd030936>
- Ryken, A., Bearup, L. A., Jefferson, J. L., Constantine, P., & Maxwell, R. M. (2020). Sensitivity and model reduction of simulated snow processes: Contrasting observational and parameter uncertainty to improve prediction. *Advances in Water Resources*, *135*, 103473. <https://doi.org/10.1016/j.advwatres.2019.103473>
- Salamon, P., Fernández-García, D., & Gómez-Hernández, J. J. (2006). A review and numerical assessment of the random walk particle tracking method. *Journal of Contaminant Hydrology*, *87*(3–4), 277–305. <https://doi.org/10.1016/j.jconhyd.2006.05.005>
- Shields, C. A., & Kiehl, J. T. (2016). Atmospheric river landfall-latitude changes in future climate simulations. *Geophysical Research Letters*, *43*(16), 8775–8782. <https://doi.org/10.1002/2016gl070470>
- Shields, C. A., Rutz, J. J., Leung, L.-Y., Ralph, F. M., Wehner, M., Kawzenuk, B., et al. (2018). Atmospheric River Tracking Method Intercomparison Project (ARTMIP): Project goals and experimental design. *Geoscientific Model Development*, *11*(6), 2455–2474. <https://doi.org/10.5194/gmd-11-2455-2018>
- Siirila, E. R., & Maxwell, R. M. (2012). Evaluating effective reaction rates of kinetically driven solutes in large-scale, statistically anisotropic media: Human health risk implications: Risk implications of kinetic solutes. *Water Resources Research*, *48*(4). <https://doi.org/10.1029/2011wr011516>
- Siirila, E. R., Navarre-Sitchler, A. K., Maxwell, R. M., & McCray, J. E. (2012). A quantitative methodology to assess the risks to human health from CO<sub>2</sub> leakage into groundwater. *Advances in Water Resources*, *36*, 146–164. <https://doi.org/10.1016/j.advwatres.2010.11.005>
- Siirila-Woodburn, E. R. (2023). erwoodburn/Siirila-Woodburn-et-al.-WRR-2023: V0 (Version v0). [Dataset]. Zenodo (January 17). <https://doi.org/10.5281/zenodo.7545440>
- Siirila-Woodburn, E. R., Fernández-García, D., & Sanchez-Vila, X. (2015). Improving the accuracy of risk prediction from particle-based breakthrough curves reconstructed with kernel density estimators. *Water Resources Research*, *51*(6), 4574–4591. <https://doi.org/10.1002/2014wr016394>
- Siirila-Woodburn, E. R., & Maxwell, R. M. (2015). A heterogeneity model comparison of highly resolved statistically anisotropic aquifers. *Advances in Water Resources*, *75*, 53–66. <https://doi.org/10.1016/j.advwatres.2014.10.011>

- Siirila-Woodburn, E. R., Rhoades, A. M., Hatchett, B. J., Huning, L. S., Szinai, J., Tague, C., et al. (2021). A low-to-no snow future and its impacts on water resources in the western United States. *Nature Reviews Earth & Environment*, 2(11), 800–819. <https://doi.org/10.1038/s43017-021-00219-y>
- Siirila-Woodburn, E. R., Sanchez-Vila, X., & Fernández-García, D. (2015). On the formation of multiple local peaks in breakthrough curves. *Water Resources Research*, 51(4), 2128–2152. <https://doi.org/10.1002/2014wr015840>
- Skamarock, W. C., & Klemp, J. B. (2008). A time-split nonhydrostatic atmospheric model for research and NWP applications. *Journal of Computational Physics*, 227(7), 3465–3485. <https://doi.org/10.1016/j.jcp.2007.01.037>
- Skamarock, W. C., Klemp, J. B., Dudhia, J., Gill, D. O., Barker, D., Duda, M. G., et al. (2008). *A description of the advanced research WRF version 3*, NCAR Technical Note NCAR/TN-475+STR. University Corporation for Atmospheric Research. <https://doi.org/10.5065/D68S4MVH>
- Ullrich, P. A., & Zarzycki, C. M. (2017). TempestExtremes: A framework for scale-insensitive pointwise feature tracking on unstructured grids. *Geoscientific Model Development*, 10(3), 1069–1090. <https://doi.org/10.5194/gmd-10-1069-2017>
- Ullrich, P. A., Zarzycki, C. M., McClenny, E. E., Pinheiro, M. C., Stansfield, A. M., & Reed, K. A. (2021). TempestExtremes v2.1: A community framework for feature detection, tracking, and analysis in large datasets. *Geoscientific Model Development*, 14(8), 5023–5048. <https://doi.org/10.5194/gmd-14-5023-2021>
- Vahmani, P., & Jones, A. D. (2017). Water conservation benefits of urban heat mitigation. *Nature Communications*, 8(1), 1072. <https://doi.org/10.1038/s41467-017-01346-1>
- Vahmani, P., Jones, A., & Particola, C. (2019). Interacting implications of climate change, population dynamics, and urban heat mitigation for future exposure to heat extremes. *Environmental Research Letters*, 14(8), 084051. <https://doi.org/10.1088/1748-9326/ab28b0>
- Wilusz, D. C., Harman, C. J., Ball, W. P., Maxwell, R. M., & Buda, A. R. (2020). Using particle tracking to understand flow paths, age distributions, and the paradoxical origins of the inverse storage effect in an experimental catchment. *Water Resources Research*, 56(4). <https://doi.org/10.1029/2019wr025140>
- Yang, C., Zhang, Y.-K., Liang, X., Olschanowsky, C., Yang, X., & Maxwell, R. (2021). Accelerating the Lagrangian particle tracking of residence time distributions and source water mixing towards large scales. *Computers & Geosciences*, 151, 104760. <https://doi.org/10.1016/j.cageo.2021.104760>
- Zhou, Y., O'Brien, T. A., Ullrich, P. A., Collins, W. D., Patricola, C. M., & Rhoades, A. M. (2021). Uncertainties in atmospheric river lifecycles by detection algorithms: Climatology and variability. *Journal of Geophysical Research*, 126(8). <https://doi.org/10.1029/2020jd033711>
- Zhu, Y., & Newell, R. E. (1994). Atmospheric rivers and bombs. *Geophysical Research Letters*, 21(18), 1999–2002. <https://doi.org/10.1029/94gl01710>